ARTICLE

Effect of ECAP temperature on precipitation and strengthening mechanisms of Mg–9Al–1Si alloys

Pengwen Zhou, Hongxia Wang,[a] Huihui Nie, Weili Cheng,[b] Xiaofeng Niu, Zhiwen Wang, and Wei Liang
Shanxi Key Laboratory of Advanced Magnesium Based Materials, College of Materials Science and Engineering, Taiyuan University of Technology, Taiyuan 030024, China

(Received 14 February 2018; accepted 20 April 2018)

The effect of equal-channel angular pressing (ECAP) at various temperatures (310, 330, and 350 °C) on precipitations and strengthening mechanisms of Mg–9Al–1Si alloys was investigated. The results indicated that the average grain size decreased gradually with decreasing of ECAP temperature. The distribution of the Mg_2Si phase changed a little when the ECAP temperature increased. However, the different morphologies of β-$Mg_{17}Al_{12}$ phase were observed, including continuous and uncontinuous precipitation of particles at 310 and 350 °C. The continuous β-$Mg_{17}Al_{12}$ phase was hardly found and the refined β-$Mg_{17}Al_{12}$ phase was distributed dispersedly in the matrix at 330 °C. Thus, the mechanical properties of the Mg–9Al–1Si alloy was optimum: ultimate tensile strength and elongation were ~350.8 MPa and ~14.77%, respectively. It can be deduced that both grain refinement strengthening and precipitation strengthening play significant roles in strength increment of the alloy during the ECAP process. However, precipitation strengthening is the predominant mechanism.

I. INTRODUCTION

Magnesium (Mg) and its alloys have attracted much attention due to their low density, high specific strength, excellent damping capacities, good machinability, and excellent castability.[1,2] However, the strength of Mg alloys is usually improved at the expense of elongation (EL).[3] It is still a challenge to obtain the best overall mechanical properties, with a balance in strength and ductility.[4]

Equal-channel angular pressing (ECAP) is regarded as one of the most effective ways of severe plastic deformation to improve mechanical properties of materials. A large deformation results in grain refinement and modification of the second phase of alloys.[5–9] Previous study has shown that grain refinement strengthening occurs together with precipitation strengthening, which is propitious to enhance mechanical properties of the Al–Zn–Mg–Cu alloy during the ECAP process.[7] Mg possesses a hexagonal close-packed crystal structure with a few slip systems, and some of them are difficult to be activated at room temperature. Consequently, Mg and its alloys are usually deformed at a certain temperature.[10–12] Krajňák et al.[13] found that increasing ECAP temperature in AX41 with large grain size led to poor performance. However, Hong et al.[14] reported that excellent mechanical properties in the extruded Mg–Gd–Y–Zr alloy at 400 °C, which possessed the bimodal grain structure with coarse grain and fine grain regions were obtained. Besides, the increasing of ECAP temperature is beneficial to both the diffusion rate of various elements and the nucleation and the growth rate of precipitation in alloys,[15] so the morphology and distribution of precipitation are affected in alloys. Furthermore, various influences of ECAP temperature on the second phase with different melting points have been studied.[16] Thus, it can be seen that ECAP temperature affects both grain refinement strengthening and precipitation strengthening. Cheng et al.[17] found that Mg_2Sn phase with low melting point precipitated in Mg–8Sn–6Zn–2Al alloys during ECAP process. Afifi et al.[9] showed that the η′ phase was refined during the ECAP process in Zn–Mg alloys. At the same time, the η phase formed in the process. Shaeri et al.[7] revealed that the precipitation strengthening played the most important role in the improvement of mechanical properties about ECAPed Al-7075. Kang et al.[3] found that the effect of grain refinement strengthening is far greater than the precipitation strengthening in extruded AZ91–0.5Ca alloys. Hence, the effect of grain refinement strengthening and precipitation strengthening mechanism is different at various alloy series.[3,9,17] Nevertheless, there is no deep research on the strengthening mechanism of the alloy with different types of second phase and bimodal grain structure. Wang et al.[8] attained a uniform fine grain structure with the homogeneously dispersed $Mg_{17}Al_{12}$ phase and Mg_2Si phase in

Address all correspondence to these authors.
[a]e-mail: wanghxia1217@163.com
[b]e-mail: chengweili7@126.com
DOI: 10.1557/jmr.2018.137

ECAPed Mg–Al–Si alloys at 300 °C. The strength under both room and high temperature of the alloy were greatly improved. However, the strengthening mechanism was not sufficiently analyzed in their reports. It is to be noted that there has been few reports about strengthening mechanism in the Mg–Al–Si alloy with the bimodal grain structure.[8,18]

Accordingly, the Mg–9Al–1Si alloys with different second phases ($Mg_{17}Al_{12}$ phase and Mg_2Si phase) are selected to investigate the effect of ECAP temperature on the grain and precipitation in the present paper. The interaction mechanism of the grain refinement strengthening and precipitation strengthening in the alloy during the ECAP process was also reported in this paper.

II. EXPERIMENTAL MATERIALS AND PROCEDURES

The Mg–9Al–1Si (wt%) alloy was prepared from pure Mg ingot (99.99 wt%), Al ingot (99.99 wt%), and Al–30% (wt%) Si master alloy. The experimental alloys were melted in an electrical resistance furnace under atmosphere of protective SF_6 + CO_2 gas. Pure Mg and appropriate amounts of pure aluminum were added into a steel crucible which was preheated at 400 °C, then the temperature was increased to 720 °C and held for 20 min. The melting temperature increased approximately 730 °C, Al–30% Si master alloys were mixed to the melt. The melt was stirred mechanically and mixed completely at 700 °C. After that, to improve the morphology and distribution of the second phase, ultrasonic vibration (UV) was used with 1200 W for 20 min.[19] The melt was casted into an iron mold with the inner diameter of 40 mm which was preheated to 250 °C. The chemical composition of the resulting billets was determined through inductively coupled plasma spectrometry to be Mg–8.96Al–1.01Si (wt%), which was very close to their respective expected values. Prior to ECAP, the treatment (T4) of billets was carried out at 420 °C for 24 h and water quenched. The billets (12 × 12 × 63 mm) were pressed through an ECAP die with an angle between the intersecting channels of $\Phi = 90°$, an outer arc of curvature of $\Psi = 20°$ and the channel had a quadrate (12 × 12 mm) cross-section throughout the die. The ECAP was carried out at three temperatures (310, 330, and 350 °C) for two passes, the samples were pressed at a rate of 1.0 mm/min by route Bc (i.e., the samples were rotated around clockwise by 90° between each pass).[8,20]

The sample was analyzed by using a Leica DM2500M optical microscope (OM; Leica Microsystems, Heidelberg, Germany). The size and morphology of the second phase were observed by using a TESCAN Mira3 LMH scanning electron microscope (SEM; TESCAN, Brno, Czech Republic) and a JEOL 2100F transmission electron microscope (TEM; JEOL Ltd., Tokyo, Japan). At least ten images were used to count the diameter and number of the second phase and grain size by Image-Pro Plus software (Media Cybernetics, Rockville, Maryland). To characterize the second phases, X-ray diffraction (XRD) analysis was performed by using a TD-3500 (Dandong Ray Instrument Co. Ltd., Dandong, China) equipped with a Cu anode at a scanning velocity of 6°/min and range of 20°–80°. Before the analysis, the sample surface was chemically etched by using the solution including 10 mL H_2O, 10 mL acetic acid, 90 mL ethyl alcohol, and 4.2 g picric acid.

Tensile tests were conducted on a DNSl00 test machine with a speed of 0.5 mm/min. The samples with a gauge length of 15 mm and a cross section of 2.0 × 1.5 mm were selected in tensile tests.

III. RESULTS AND DISCUSSION

The OM microstructure shown in Fig. 1(a) indicates the Mg_2Si phase with coarse Chinese script shape clusters along the grain boundaries, and the average grain size ($\bar{d}$) of the Mg–9Al–1Si alloy under the UV + T4 (UV during the molten state and T4 treatment) condition is observed to be ~203 μm. Figure 1(b) presents the XRD pattern of the UV + T4 condition alloy, showing two intermetallic phases (Mg_2Si, $Mg_{17}Al_{12}$) and a matrix α-Mg phase prior to the ECAP process, respectively. However, the diffraction intensity peak of the $Mg_{17}Al_{12}$ phase in XRD was almost negligible due to the T4 treatment. This demonstrated that a large amount of eutectic $Mg_{17}Al_{12}$ phase had been dissolved in the matrix,[21] and the content of $Mg_{17}Al_{12}$ was low in the pretreated alloy which is not observed in the OM [Fig. 1(a)]. On the contrary, the T4 treatment has little effect on the Mg_2Si phase owing to its high melting point.[1]

Figure 2 illustrates the SEM-EDS of the ECAPed Mg–9Al–1Si alloy at 310 °C and XRD patterns of ECAPed Mg–9Al–1Si alloys at various temperatures [310 °C—(b), 330 °C—(c), and 350 °C—(d)]. This reveals that the Mg_2Si phase is fragmented from coarse Chinese script shape to rod-like in Fig. 2(a). In addition, the white granular $Mg_{17}Al_{12}$ phases precipitated along grain boundaries and at the interface between Mg_2Si phase and α-Mg matrix, and a small amount of $Mg_{17}Al_{12}$ phases were observed in the position where the crack formed in the Mg_2Si phase. Compared with the XRD pattern of pretreated (UV + T4) in Fig. 1(b), the corresponding β-$Mg_{17}Al_{12}$ peak intensity significantly increases, which indicates that ECAP promoted the precipitation of the $Mg_{17}Al_{12}$ phase from the α-Mg matrix in Figs. 2(b)–2(d).[15] Moreover, it can be seen from Fig. 2(c) that the peak of the $Mg_{17}Al_{12}$ phase was strongest, which indicates that the maximum amount of $Mg_{17}Al_{12}$ particles is obtained at 330 °C.

Figure 3 shows the OM and SEM microstructures of the ECAPed alloy with fractured Chinese script-shaped Mg_2Si particles. The grain size ($\bar{d}$) of ECAPed alloys at

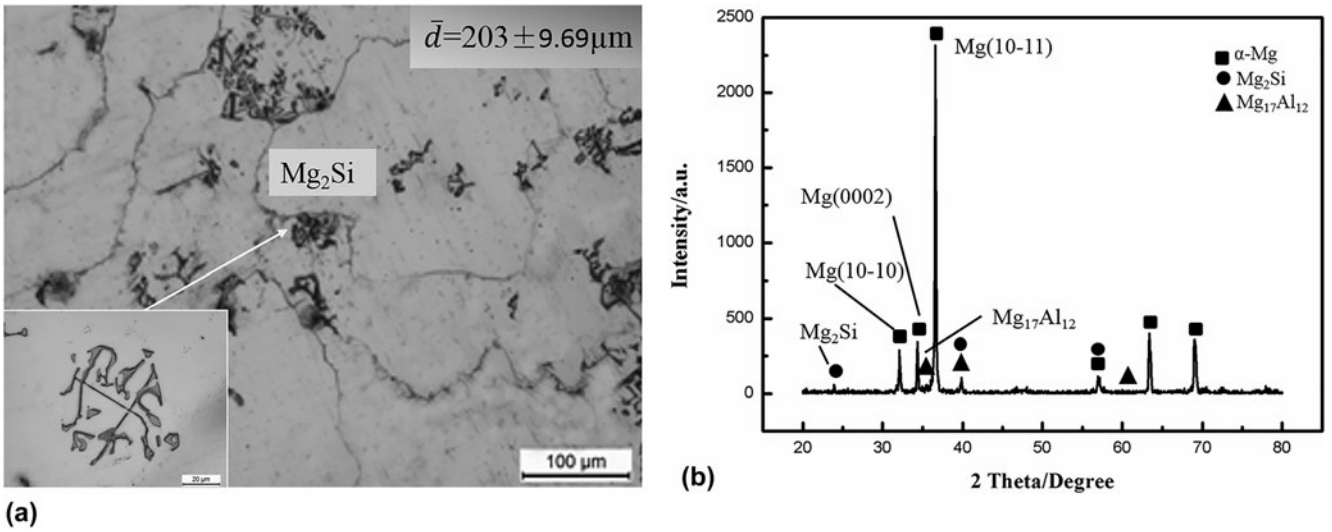

FIG. 1. OM (a) and XRD patterns (b) of pretreated (UV + T4) Mg–9Al–1Si alloys.

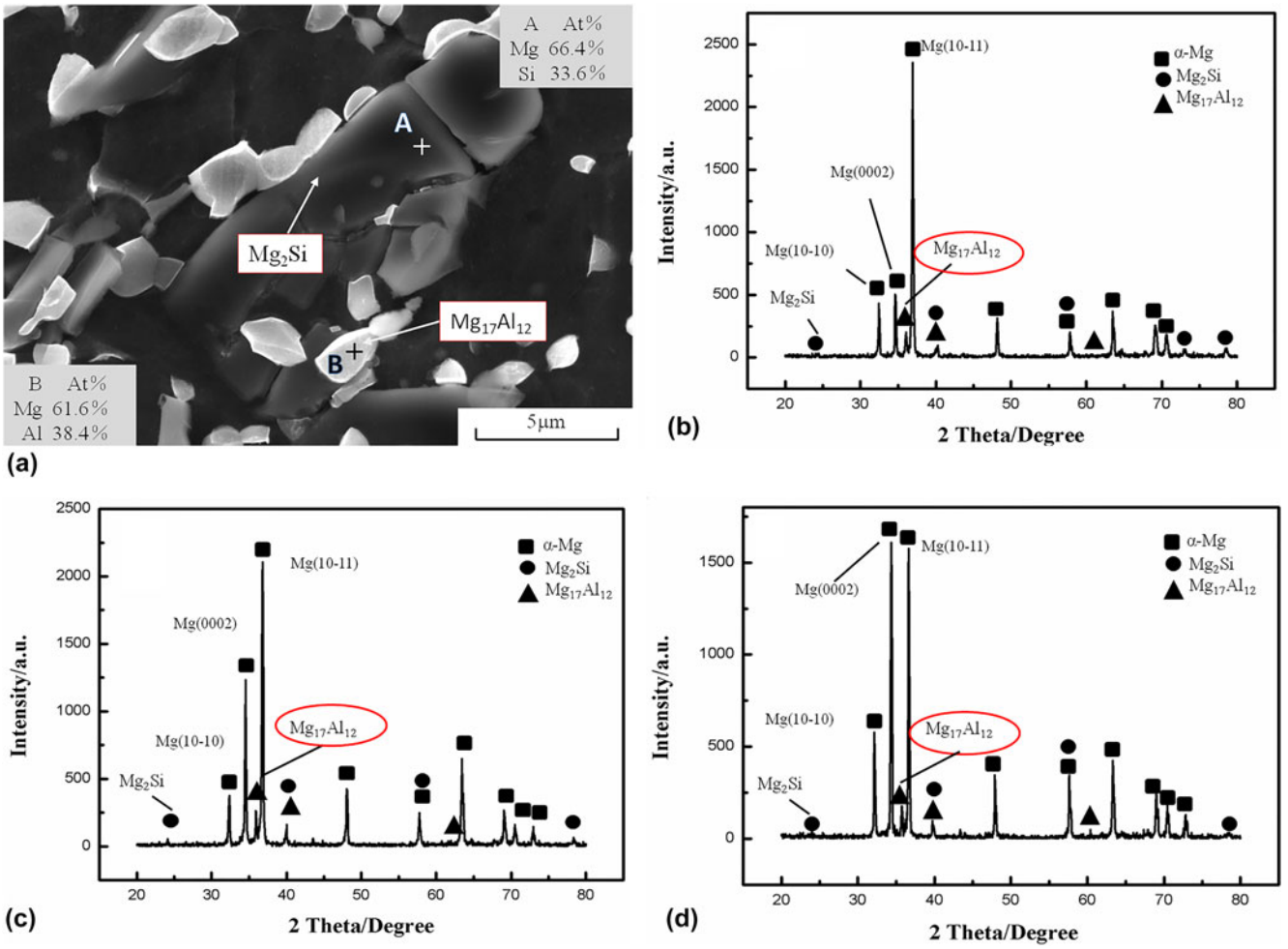

FIG. 2. SEM-EDS of the ECAPed Mg–9Al–1Si alloy at 310 °C (a) and XRD patterns of different ECAP temperatures: 310 °C (b), 330 °C (c), and 350 °C (d).

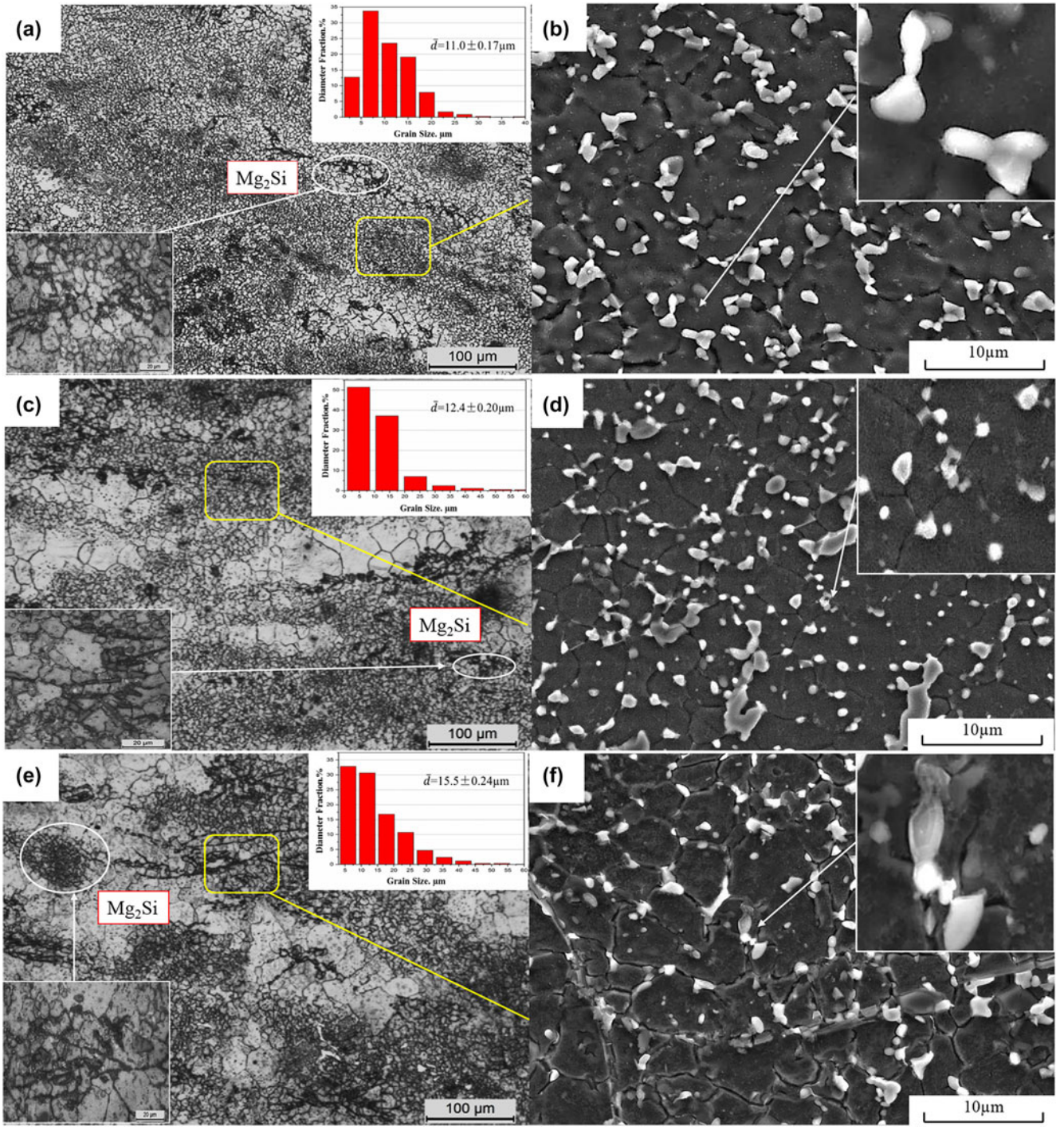

FIG. 3. OM and SEM of the Mg–9Al–1Si alloy ECAPed at different temperatures by two passes: (a and b) 310 °C, (c and d) 330 °C, (e and f) 350 °C.

310 °C has been refined effectively. The $\bar{d}$, illustrated by shown in the distribution bar graph of grain size in Fig. 3(a), decreased to ~11.0 μm and the dynamically recrystallized (DRXed) grain is homogeneous distribution. Furthermore, it can be seen that the Mg_2Si phase was fully broken down into finer particles. Meanwhile, a large number of fine $Mg_{17}Al_{12}$ phases precipitated along the grain boundaries. Besides, a considerable part of $Mg_{17}Al_{12}$ particles are connected to each other, which leads to a micro-aggregation. The average diameter and quantity of precipitation were 1.435 (±0.025) μm and 126.3, respectively. The detailed values are given in Table I. As demonstrated in Fig. 3, it is obviously observed that the grain size in DRXed fine grain regions

TABLE I. Mechanical properties of the ECAP Mg–9Al–1Si alloy at different temperatures and details of the second phase particle.

Alloy	Pretreated	2-Pass ECAP temperature (°C)	Mechanical properties			Second-phase (mean)	
			TYS (MPa)	TUS (MPa)	EL (%)	Number X	Diameter d (μm)
Mg–9Al–1Si	UC + T4	310	194	300.0	13.87	126.3	1.435 (±0.025)
		330	290	350.8	14.77	231.9	0.930 (±0.015)
		350	225	271.3	10.18	124.4	1.319 (±0.031)

at 330 °C, which was smaller than that at 310 °C. It is worth noting that a little coarse grain regions appeared at 330 °C, so there was a slight fluctuation in the average grain size $\bar{d}$ (~12.4 μm). Otherwise, the size of the Mg_2Si particle changed a little but it tends to be a homogeneous distribution. However, the precipitated particle of the $Mg_{17}Al_{12}$ phase was refined in size and incremented in number, majority of uncontinuous $Mg_{17}Al_{12}$ phases precipitated along the grain boundaries. As shown in Fig. 3(b) and Table I, the average size (d) of precipitation decreases sharply to 0.930 (±0.015) μm and the amount increases hastily to 231.9 with ECAP temperature elevates from 310 to 330 °C, which is in accordance with the strongest diffraction intensity peak presented in Fig. 2(c). The fraction of coarse grain region increment and the grain sizes of both coarse grain regions and fine grain regions increased, resulting in the increase of $\bar{d}$ (~15.5 μm) at 350 °C. The dispersion degree of the Mg_2Si particle decreased [Fig. 3(e)] and the size of the $Mg_{17}Al_{12}$ phase increased slightly, it deserves to be mentioned that the micro-aggregation of particles reappeared [Fig. 3(f)]. In this case, the average size of the $Mg_{17}Al_{12}$ phase increases to 1.319 (±0.031) μm and the average number significantly declines to 124.4 (Table I).

The ECAP temperature range in this paper is higher than the recrystallization temperature of Mg alloys,[23,24] which results in the dynamical recrystallization of the Mg–9Al–1Si alloy. However, the coarse grain regions appear accompanied by the increase of ECAP temperature. The results above can be explained that, in the premise of other experimental conditions are constants, the high ECAP temperature can accelerate the rate of atomic diffusion and increase the rate of grain growth about recrystallization.[15] The matrix grain of the alloy grows slowly after nucleation and nucleation and dynamically precipitated second phase particles pinned grain boundary, which leads to the smallest average grain size of the alloy without coarse grain regions at 310 °C.[25] The alloys ECAPed at 330 °C exhibit a typical bimodal grain structure, which are composed of coarse grain region and fine grain region.[10,12] Grains grow up obviously in coarse grain regions because the growth rate of the grain is accelerated. Besides, the coarse grain region with little precipitation is affected a little by the particle stimulating nucleation mechanism.[26] The precipitation does not effectively hinder the migration of the grain boundary. On the contrary, the diffusion rate of elements and the growth rate of precipitation increase accompanied by the increase of temperature.[15] In addition, grain boundaries in DRXed regions are pinned by numerous fine precipitations. Thus, the grain size in the fine grain regions at 330 °C is smaller than that in ECAPed at 310 °C. Some precipitations merge and grow in alloys at 350 °C, which can be attributed to the decreased nucleation sites and accelerated atomic diffusion rate.[8] Thus, the pinning effect was weaken, and coarse grain regions sharply increased and grains in the fine grain regions grow up obviously, which results in the increase of average grain size in the alloy.

Numerous fine $Mg_{17}Al_{12}$ phases precipitate during the ECAP process.[15] As shown in Fig. 3, the morphology and distribution of the particles changed with the temperature increase. Despite that the fine grain with more grain boundaries can provide more nucleation sites, there are less precipitation by ECAP at 310 °C. The aggregation of the $Mg_{17}Al_{12}$ phase and large size $Mg_{17}Al_{12}$ phase particles appeared during the ECAP process, which originated from the slow diffusion rate of Al elements in the matrix and a small capability of nucleation of the $Mg_{17}Al_{12}$ phase.[26] The refined $Mg_{17}Al_{12}$ precipitation distribute dispersively during the ECAP process at 330 °C. The diffusion rate of Al in the Mg matrix and the nucleation rate of the $Mg_{17}Al_{12}$ phase accelerate, and the $Mg_{17}Al_{12}$ phase is attained abundant nucleation sites in the fine grain regions can explain these phenomena.[21] Besides, there is no time for the $Mg_{17}Al_{12}$ phase to grow up at 330 °C during the ECAP process. Particle connection does not appear. However, the mean grain size increases and the amount of nucleation sites of the $Mg_{17}Al_{12}$ phase decrease at 350 °C. Meanwhile, $Mg_{17}Al_{12}$ phase particles growth and cohesion appear again during the ECAP process, which is attributed to the increase of nucleation and growth rate of the $Mg_{17}Al_{12}$ phase. Therefore, the alloy with smallest average sizes and largest amount of the $Mg_{17}Al_{12}$ phase were obtained by ECAP at 330 °C. In addition, as shown in Figs. 3(a), 3(c), and 3(e), the Mg_2Si phase is obviously shredded during the ECAP process, but its dispersion is affected a little owing to its high melting point.[22]

The stress–strain curves of the ECAPed Mg–9Al–1Si alloy at different temperatures are shown in Fig. 5. The corresponding performance values are shown in Table I. Figure 5 and Table I indicate that the mechanical properties of the Mg–9Al–1Si alloy are strongly affected

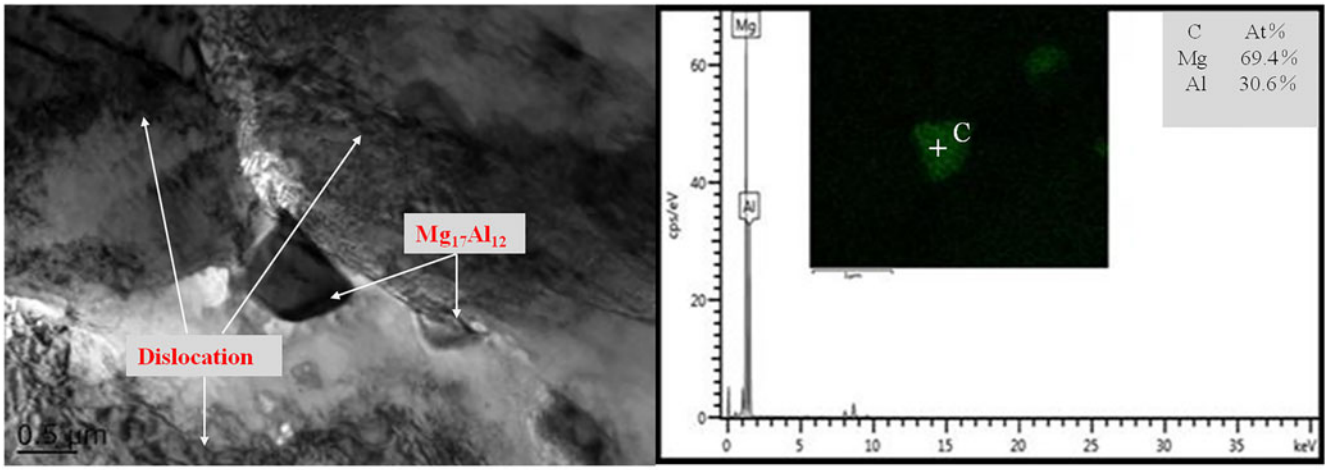

FIG. 4. Micrographs of TEM (a) and corresponding STEM (b) about the $Mg_{17}Al_{12}$ phase ECAPed at 330 °C.

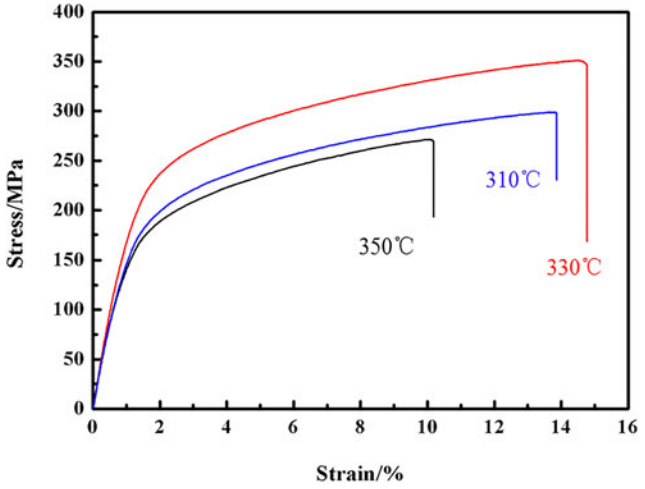

FIG. 5. Tensile stress–strain curve of the Mg–9Al–1Si alloy ECAPed at different temperatures.

by the temperature of ECAP. The ultimate tensile strength (UTS) and EL of the present alloy at 310 °C are ~300 MPa, and ~13.87%, respectively, the tensile yield strength (TYS) is ~194 MPa. By comparison, the UTS and EL of the alloy at 350 °C drop by 28.7 MPa and 3.69%, respectively. It can be concluded that the optimum mechanical properties of the ECAPed Mg–9Al–1Si alloy are attained at 330 °C. Comparing with that ECAPed at 310 °C and 350 °C, the TYS increased by ~49.48% and ~28.29%, respectively, and the UTS of the alloy increased by ~50.8 MPa and ~79.5 MPa. In addition, the EL (~14.77%) is the highest in the three temperatures of ECAP.

According to the Hall–Petch effect,[27] $\sigma_y = \sigma_0 + kd^{1/2}$, where σ_y is the TYS, σ_0 and k are the material constants. Then, the strength of the material is inversely proportional to the grain size. The finer the grain is, the higher the strength of the material is. As observed in present investigation, mechanical properties of the alloys with the smallest average grain sizes were not the most favorable. It originates from the high content of the second phase in the ECAPed Mg–9Al–1Si alloy.[18] The second phase retards the grain boundary migration and the movement of dislocation in the tensile test process,[6] as can be seen in Fig. 4. The strength increments stem from the effect of grain refinement strengthening and precipitation strengthening.[22] The gap of grain refinement strengthening at different temperatures can be estimated as[3]

$$\begin{aligned}\Delta\sigma_{g1} &= k\left(\bar{d}_{330^\circ C}^{-1/2} - \bar{d}_{310^\circ C}^{-1/2}\right)\\ \Delta\sigma_{g2} &= k\left(\bar{d}_{330^\circ C}^{-1/2} - \bar{d}_{350^\circ C}^{-1/2}\right)\end{aligned}, \quad (1)$$

where $\Delta\sigma_{g1}$ is the difference of grain refinement strengthening between 330 and 310 °C and $\Delta\sigma_{g2}$ is the difference of grain refinement strengthening between 330 and 350 °C. Accordingly, the calculated $\Delta\sigma_{g1}$ and $\Delta\sigma_{g2}$ are −5 MPa and 16.2 MPa, respectively. The usual model used to determine precipitation strengthening of the Mg alloy is as follows[7,15,21,22]:

$$\Delta\sigma_p = 0.4MGb\ln(d/b)/\lambda\pi(1-V)^{1/2}, \quad (2)$$

where d is the mean size of precipitates, λ is the average distance between them, b is the Burgers vector of dislocations, and all of V, π, M, and G are constants for the Mg alloy. In addition, the gap of precipitation strengthening at different temperatures can be estimated as

$$\begin{aligned}\Delta\sigma_{p1} &= \Delta\sigma_{p330} - \Delta\sigma_{p310^\circ C}\\ \Delta\sigma_{p2} &= \Delta\sigma_{p300^\circ C} - \Delta\sigma_{p350^\circ C}\end{aligned}, \quad (3)$$

where $\Delta\sigma_{p1}$ is the difference of precipitation strengthening between 330 and 310 °C and $\Delta\sigma_{p2}$ is the difference of

precipitation strengthening between 330 and 350 °C. Accordingly, the calculated $\Delta\sigma_{p1}$ and $\Delta\sigma_{p2}$ are 45.7 MPa and 46.5 MPa, respectively. It can be concluded that the more the precipitates disperse, the higher tensile and YS would it attain. In the SEM field of the alloy in Fig. 3, the smaller the second phase particles size d and distance λ are, the smaller the number of the second phase X is. It can be regarded λ as the number of the second phase in the same field of view (SEM). The distributions of Mg_2Si at different ECAP temperatures have not obvious discrepancy. Therefore, K can be described by the following relationship, which means the ratio of average number X and the mean size d of $Mg_{17}Al_{12}$ phase particles:

$$K = X/d \quad . \tag{4}$$

Equation (4) reveals that the larger the value of K is, the more obvious the precipitation strengthening effect is.[17] In fact, the values of K are 88.05 and 94.01 for the ECAPed alloy at 310 °C and 350 °C, respectively. The highest value of K is 248.39 for the ECAPed alloy at 330 °C. It is worth noting that, according to the Eqs. (1) and (3), the value of $\Delta\sigma_{p1}$ is much higher than that of $\Delta\sigma_{g1}$. Therefore, the effect of precipitation strengthening is the most remarkable for the ECAPed alloy at 330 °C. It may be that the dislocation strengthening and calculated deviation are responsible for the left part of strengthen.[28,29]

In addition, the average grain size of the alloy ECAPed at 310 and 330 °C is almost similar. It is clear that the plasticity of the present alloy ECAP at 310 °C is smaller than that at 330 °C. At the same time, a small amount of coarse grain regions and fine grain regions with ultrafine grains produced in the ECAPed alloy at 330 °C. Previous studies reported that the bimodal grain structure can promote the plasticity: Zheng et al.[30] reported that the appropriate coarse grains (>1 μm) accommodate strains preferentially and are effective in storing dislocations, Moreover, the bimodal grain structure may cause the deformation of grains via complex strain paths, which is also beneficial for dislocation storage.[22] Hong et al.[14] also found that a small amount of fine recrystallized grains acted as lubricant between coarse grains, which could adjust deformation and guarantee a good elongation. Hence, the plasticity of the ECAPed alloy at 330 °C is superior to that at 310 °C. The size of grain in coarse grain regions of the ECAPed alloy at 350 °C is larger than that at 330 °C, which caused a nonuniform deformation within one coarse grain and resulted in stress concentration on the grain boundary. As a result, the stress concentration caused microcracks at the coarse grain boundary during the tensile tests, which results in poor ductility of the Mg–9Al–1Si alloy.[12]

Totally, the grain size of the ECAPed alloy at 330 °C is slightly larger than that at 310 °C. However, the UTS and EL are both higher than that at 310 °C. The grain size of the ECAPed alloy at 350 °C is larger than that at 330 °C, but its UTS and EL are both lower than that at 330 °C. It can be concluded that compared with grain refinement strengthening, precipitation strengthening is the dominant strengthening mechanism during the ECAP process at various temperatures.

IV. CONCLUSION

According to the results obtained, the following conclusions can be drawn:

(1) Mg_2Si phases are fragmented in the ECAP process, but the dispersion does not change a lot. On the contrary, some remarkable changes take place in the precipitated $Mg_{17}Al_{12}$ phase. Numerous fine $Mg_{17}Al_{12}$ phases solely precipitate at 330 °C, and the phenomenon of particle connection occurs in the ECAPed alloy at 310 and 350 °C. It stems from the influence of temperature on the diffusion rate of elements and the precipitation behavior of the second phase with low melting points.

(2) During the ECAP process, the grains are refined and the $Mg_{17}Al_{12}$ phases precipitate from the matrix of the Mg–9Al–1Si alloy obviously. In fact, both grain refinement strengthening and precipitation strengthening play significant roles in strength increment of ECAPed alloys. However, the analyses about the contributions of the two strengthening mechanisms indicate that the effect of grain refinement strengthening is less remarkable than the precipitation strengthening during the ECAP process at various temperatures.

(3) The most favorable mechanical properties of the ECAPed Mg–9Al–1Si alloy at 330 °C was attained. The UTS of it is 350.8 MPa, which is much higher than that at 350 and 310 °C. It can be explained that the presence of the fine dispersion of the second phase in the microstructure leads to the result above. The EL is also the highest (14.77%) at 330 °C, which results from the bimodal grain structure.

ACKNOWLEDGMENTS

This work was financially supported by Natural Science Foundation of Shanxi Province (201701D121045); National Natural Science Foundation of China (51771129, 51301118, and 51404166); and Shanxi Key Laboratory of Advanced Magnesium-based Materials, Taiyuan University of Technology (AMM-2017-12).

REFERENCES

1. P. Poddar, S. Bagui, K. Ashok, and A.P. Murugesanl: Experimental investigation on microstructure and mechanical properties of gravity-die-cast, magnesium alloys. *J. Alloys Compd.* **695**, 895 (2016).
2. T. Krajňák, P. Minárik, and J. Stráská: Influence of equal channel angular pressing temperature on texture, microstructure and

mechanical properties of extruded AX41 magnesium. *J. Alloys Compd.* **705**, 273 (2017).
3. J.W. Kang, X.F. Sun, K.K. Deng, F.J. Xu, X. Zhang, and Y. Bai: High strength Mg–9Al serial alloy processed by slow extrusion. *Mat. Sci. Eng., A*, **697**, 211 (2017).
4. J.M. Hu, J. Teng, X.K. Ji, D.F. Fu, W.G. Zhang, and H. Zhang: Enhanced mechanical properties of an Al–Mg–Si alloy by repetitive continuous extrusion forming process and subsequent aging treatment. *Mat. Sci. Eng., A* **695**, 35 (2017).
5. A. Vinogradov: Effect of severe plastic deformation on tensile and fatigue properties of fine-grained magnesium alloy ZK60. *J. Mater. Res.* **32**, 1 (2017).
6. P.C. Yadav, S. Sahu, A. Subramaniam, and S. Shekhar: Effect of heat-treatment on microstructural evolution and mechanical behaviour of severely deformed Inconel 718. *Mat. Sci. Eng., A*. **715**, 295 (2018).
7. M.H. Shaeri, M. Shaeri, M. Ebrahimi, M.T. Salehi, and S.H. Seyyedein: Effect of ECAP temperature on microstructure and mechanical properties of Al–Zn–Mg–Cu alloy. *Prog. Nat. Sci.: Mater.* **26**, 182 (2016).
8. W.H. Wang, H.X. Wang, Y.M. Liu, H.H. Nie, and W.L. Cheng: Effect of SiC nanoparticles addition on the microstructures and mechanical properties of ECAPed Mg9Al–1Si alloy. *J. Mater. Res.* **32**, 615 (2017).
9. M.A. Afifi, P.H.R. Pereira, Y.C. Wang, Y.W. Wang, S.K. Li, and T.G. Langdon: Effect of ECAP processing on microstructure evolution and dynamic compressive behavior at different temperatures in an Al–Zn–Mg alloy. *Mat. Sci. Eng., A* (2016).
10. J. Zhang, G.Q. Xi, X. Wan, and C. Fang: The dislocation-twin interaction and evolution of twin boundary in AZ31 Mg alloy. *Acta Mater.* **133**, 208 (2017).
11. X.J. Wang, D.K. Xu, R.Z. Wu, X.B. Chen, Q.M. Peng, L. Jin, Y.C. Xin, Z.Q. Zhang, Y. Liu, X.H. Chen, G. Chen, K.K. Deng, and H.Y. Wang: What is going on in magnesium alloys? *J. Mater. Sci. Technol.* **34**, 245 (2017).
12. S.Q. Zhu and S.P. Ringer: On the role of twinning and stacking faults on the crystal plasticity and grain refinement in magnesium alloys. *Acta Mater.* **144**, 365 (2018).
13. T. Krajňák, P. Minárik, J. Stráská, K. Máthis, R. Kužel, and M. Janeček: Influence of equal channel angular pressing temperature on texture, microstructure and mechanical properties of extruded AX41 magnesium. *J. Alloys Compd.* **705**, 273 (2017).
14. M. Hong, S.S.A. Shah, D. Wu, R.S. Chen, X.H. Du, N.T. Hu, and Y.F. Zhang: Ultra-high strength Mg–9Gd–4Y–0.5Zr alloy with bimodal structure processed by traditional extrusion. *Met. Mater. Int.* **22**, 1091 (2016).
15. L.L. Tang, Y.H. Zhao, R.K. Islamgaliev, C.Y.A. Tsao, R.Z. Valiev, E.J. Lavernia, and Y.T. Zhu: Enhanced strength and ductility of AZ80 Mg alloys by spray forming and ECAP. *Mat. Sci. Eng., A* **670**, 280 (2016).
16. H. Liu, J. Ju, J. Bai, J.P. Sun, D. Song, J.L. Yan, J.H. Jiang, and A. Ma: Preparation, microstructure evolutions, and mechanical property of an ultra-fine grained Mg–10Gd–4Y–1.5Zn–0.5Zr alloy. *Metals* **7**, 398 (2017).
17. W.L. Cheng, L. Tian, H.X. Wang, L.P. Bian, and H. Yu: Improved tensile properties of an equal channel angular pressed (ECAPed) Mg–8Sn–6Zn–2Al alloy by prior aging treatment. *Mat. Sci. Eng., A* **687**, 148 (2017).
18. H.X. Wang, B. Zhou, Y.T. Zhao, K.K. Zhou, W.L. Cheng, and W. Liang: Effect of Si addition on the microstructure and mechanical properties of ECAPed Mg–15Al alloy. *Mat. Sci. Eng., A* **589**, 119 (2014).
19. S. Sardar, S.K. Karmakar, and D. Das: Ultrasonic assisted fabrication of magnesium matrix composites: A review. *Mater. Today* **4**, 3280 (2017).
20. A. Veveçka, M. Cabibbo, and T.G. Langdon: A characterization of microstructure and microhardness on longitudinal planes of an Al–Mg–Si alloy processed by ECAP. *Mater. Charact.* **84**, 126 (2013).
21. J.L. Gong, W. Liang, H.X. Wang, X.G. Zhao, and L.P. Bian: Microstructure and mechanical properties of Mg–12Al–0.7Si magnesium alloy processed by equal channel angular pressing. *Mater. Sci. Forum* **42**, 1800 (2008).
22. B.G. Wang, X. Wang, J.X. Zhou, G.F. Zhang, and F. Liu: Effects of solution heat treatment on microstructure and mechanical properties of Mg–3Al–1Si–0.3Mn–*x*Sr alloy. *Mat. Sci. Eng., A* **618**, 210 (2014).
23. T.W. Wong, A. Hadadzadeh, and M.A. Wells: High temperature deformation behavior of extruded AZ31B magnesium alloy. *J. Mater. Process. Technol.* **251**, 360 (2017).
24. B. Pourbahari, H. Mirzadeh, and M. Emamy: Elucidating the effect of intermetallic compounds on the behavior of Mg–Gd–Al–Zn magnesium alloys at elevated temperatures. *J. Mater. Res.* (2017).
25. H. Zhang, T.L. Wang, and W.Y. Liu: Effect of equal channel angular pressing on microstructure and mechanical properties of Mg–Al–Si alloy. *Int. J. Plast.* **24**, 36 (2017).
26. L. Zhang, Q.D. Wang, W.J. Liao, W. Guo, B. Ye, H.Y. Jiang, and W.J. Ding: Effect of homogenization on the microstructure and mechanical properties of the repetitive-upsetting processed AZ91D alloy. *J. Mater. Sci. Technol.* **9**, 935 (2017).
27. H.H. Yu, Y.C. Xin, M.Y. Wang, and Q. Liu: Hall–Petch relationship in Mg alloys: A review. *J. Mater. Sci. Technol.* **34**, 248 (2017).
28. T. Khelfa, M.A. Rekik, J.A. Muñoz-Bolaños, J.M. Cabrera-Marrero, and M. Khitouni: Microstructure and strengthening mechanisms in an Al–Mg–Si alloy processed by equal channel angular pressing (ECAP). *Int. J. Adv. Manuf. Technol.* **95**, 1165 (2018).
29. J. Feng, H. Sun, X. Li, H. Wang, and W. Fang: Effects of Ag variations on dynamic recrystallization, texture, and mechanical properties of ultrafine-grained Mg–3Al–1Zn alloys. *J. Mater. Res.* **31**, 3360 (2016).
30. Z.J. Zheng, J.W. Liu, and Y. Gao: Achieving high strength and high ductility in 304 stainless steel through bi-modal microstructure prepared by post-ECAP annealing. *Mat. Sci. Eng., A* **680**, 426 (2016).